Differential theory of fluids below the critical temperature: Study of the Lennard-Jones fluid and of a model of C_{60}

M. Tau
Istituto Nazionale di Fisica della Materia, Dipartimento di Fisica, Università degli Studi di Parma, 43100 Parma, Italy

A. Parola, D. Pini, and L. Reatto
Istituto Nazionale di Fisica della Materia, Dipartimento di Fisica, Università degli Studi di Milano, 20133 Milano, Italy
(Received 21 December 1994)

The hierarchical reference theory (HRT) is applied to the Lennard-Jones fluid below the critical temperature T_c. This study completes a previous one performed above T_c using the same kind of approximate closure for the direct correlation function. Results for several thermodynamic quantities and for the two-particle correlations are reported and compared both with other theories and with simulation data. In the two-phase region the theory correctly yields rigorously flat isotherms; this feature allows a straightforward and accurate determination of the coexistence curve without resorting to the Maxwell construction. In the critical region our analysis is consistent with the previously developed one for $T > T_c$ and displays nontrivial critical exponents. We also study a fluid with the Girifalco model potential for C_{60}. The critical point of the liquid-vapor transition is found at $T_c = 2138$ K and $\rho_c = 0.50\,\mathrm{nm}^{-3}$. When the HRT result is supplemented with Verlet's freezing criterion a triple point is found at $T_t = 1979$ K and $\rho_t = 0.848\,\mathrm{nm}^{-3}$.

PACS number(s): 61.20.Gy, 64.70.Fx, 64.60.Fr, 64.60.Ak

I. INTRODUCTION

Nowadays several different theories are available that are able to describe with considerable accuracy the equilibrium properties of simple fluids in a wide range of thermodynamic states [1]. Nevertheless, a comprehensive theoretical description of fluids over the whole phase plane on the basis of the interparticle interaction is still an open problem: in particular, a realistic treatment both of critical behavior and of phase coexistence below the critical temperature T_c is out of the reach of current liquid-state theories since they do not take very accurately into account the long-range fluctuations that are an essential feature of such phenomena. For example, it is well known that in most theories the power-law behavior of the thermodynamic quantities at the critical point (if they do show a power-law behavior at all) is governed by mean-field or spherical model critical exponents [2]. The coexistence region is also a rather troublesome portion of the phase diagram for current liquid-state theories: in fact, none of them is able to reproduce the flat shape of the isotherms in the pressure-density plane, corresponding to infinite compressibility and constant chemical potential, which is the characteristic feature of phase coexistence. Even if it is possible to move inside this region, as in the case of some of the simplest perturbative approaches [1], the free energy remains an analytic function of its arguments and this gives rise to negative values of the isothermal compressibility and hence to mechanical instability and to the well known van der Waals loop. The region of mechanical instability is bounded by the so-called *spinodal line*, i.e., the locus of diverging compressibility. Besides, the most successful integral equation approaches, namely, the mean spherical approximation (MSA), the Percus-Yevick (PY) equation, and the hypernetted chain (HNC) equation, do not even have a solution in a certain domain inside the coexistence region. In the case of the MSA the boundary of this forbidden region coincides with the spinodal line, while in the HNC equation the compressibility remains finite on the boundary, displaying a square root branch point. The PY equation presents both kinds of behavior, respectively on the high- and low-density sides of the boundary curve [3]. It may be worth recalling that in any case the curve bounding the instability or forbidden region does not coincide with the coexistence or *binodal* line. The latter curve must be determined by performing a Maxwell construction, i.e., by explicitly requiring that the pressures and the chemical potentials of the gas and liquid phases must be equal at coexistence. This procedure, although conceptually straightforward, may require considerable effort, especially when the solution is not defined inside the two-phase region: when this is the case, two points on opposite sides of the coexistence curve must be joined by a piecemeal path so as to avoid the forbidden domain and a high degree of thermodynamic consistency of the theory is required in order to get reliable results [4]. If this condition is met, the coexistence curve can be well reproduced, at least for temperatures not too close to the critical value. However, the accuracy gets worse as one approaches the critical region, as can be seen for example in the case of the optimized cluster theory (OCT) [5]. In fact, as noted above, most of the liquid-state theories behave rather poorly in this region. Moreover, recent calculations on the Lennard-Jones fluid performed with the Zerah-Hansen (often referred to as HMSA) and the modified hypernetted chain (MHNC) equation [4,6] show that the top of the coexistence curve may even be inaccessible, since at the critical point it merges with the boundary of

the forbidden region.

It seems therefore worthwhile to revisit the phase diagram of a simple fluid below the critical temperature with the aid of a theory able to deal both with long-range fluctuations and with the strongly nonanalytic behavior of the thermodynamic quantities in the two-phase region. Such an approach, namely, the hierarchical reference theory (HRT) [7], was formulated some years ago in order to achieve a better picture of universality at the critical point and to retain, at the same time, the information about the nonuniversal properties of the fluid. To this purpose, the basic concepts of the renormalization group are developed in the framework of a liquid-state theory: in the HRT the long-wavelength part of the interaction responsible for criticality is gradually turned on so that the fully interacting system is approached through a sequence of intermediate systems in which long-range fluctuations have been strongly inhibited. The corresponding evolution of thermodynamic and correlations is described by an exact hierarchy of integro-differential equations. In particular, the first equation gives the evolution of the free energy of the system in terms of the two-particle direct correlation function [1] in momentum space $\hat{c}(k)$. A simple approximation scheme consists then in truncating the hierarchy to this equation, supplementing it with a suitable closure relation based on some ansatz for $\hat{c}(k)$. In a previous paper [8] such an approximation was applied to the Lennard-Jones fluid. In particular, it was shown that if one adopts an expression for $\hat{c}(k)$ similar to that used in the optimized random-phase approximation (ORPA) [1], the resulting theory proves to be comparable in accuracy with the best liquid-state approaches. Moreover, it provides a nontrivial description of the critical point, with critical exponents that are correct to first order in the ϵ expansion of the renormalization group [7]. However, this study was carried out only above the critical temperature of the system because at lower temperatures some difficulties in the numerical treatment of the problem set in. This was indeed a rather serious limitation since it did not allow one to investigate not only the coexistence region, but also the triple-point zone, while an accurate description of this high-density, low-temperature portion of the phase plane can now be considered as a standard requirement of a successful theory of liquids.

In the present work we have considered the extension of the previous treatment of a fluid below the critical temperature; to this aim, the numerical algorithm employed in the computation has been reformulated so as to be reliable both above and below T_c, with particular regard to the coexistence region, which is the more difficult to deal with. The results for the thermodynamic and the correlations show that in the single-phase region the theory is again as accurate as the most widely adopted approaches. Moreover, it is well defined also in the coexistence region, where it correctly preserves the convexity of the free energy. More explicitly, it will be seen that the inclusion of arbitrarily long-range fluctuations in the system removes the van der Waals loop and the region of mechanical instability; when all the fluctuations have been taken into account, the compressibility turns out to be infinite over a finite domain of the phase plane, which can then be unambiguously identified with the coexistence region. This peculiar feature of the HRT has already been pointed out in the study of a lattice gas with nearest-neighbor attraction [9] and then discussed in the more general context of the momentum space renormalization group [10]. The coexistence curve can be immediately determined up to the critical temperature as the boundary of the region of infinite compressibility without resorting to the Maxwell construction. We have applied this theory to the Lennard-Jones (LJ) potential and the agreement with the simulation data is very satisfactory. As the temperature reaches its critical value, the coexistence region correctly matches with the critical point. The latter can be located starting from both above and below T_c and compares rather well with the simulation estimates. However, the present description fails to predict the expected discontinuity of the inverse compressibility on the coexistence curve. In fact, the compressibility at coexistence is infinite in this approach and the coexistence curve merges with the spinodal line. It has already been pointed out [10] that such an unphysical property is due to the long-range behavior of correlations implied by the adopted closure relation, which assumes that the direct correlation function in momentum space $\hat{c}(k)$ is always of the Ornstein-Zernike form, while on the other hand its analyticity in the wave vector k cannot be justified inside the two-phase region, where $\hat{c}(k)$ is known to develop a discontinuity at $k = 0$ [11]. Actually, this kind of closure yields a discontinuity for the inverse compressibility at coexistence only for spatial dimension D equal to or above 4. However, we show that in $D = 3$ it is possible to get an estimate of the finite compressibility at coexistence by subtracting from the zero-wavelength value of the structure factor the anomalous contribution.

As another example of application of our theory we have considered the Girifalco model for the interatomic potential between rigid C_{60} molecules [12]. This potential has an attractive well that is considerably narrower and deeper than the LJ potential. This moves the critical point to a substantially larger packing fraction. By using Verlet's freezing criterion we also locate the freezing line and, for the C_{60} model, the triple-point temperature is only 7% below the critical one.

The paper is organized as follows. In Sec. II the theory and the adopted approximations are briefly reviewed. In Sec. III our results for the thermodynamic quantities and the correlations of a Lennard-Jones fluid are reported and discussed and a comparison both with other theories and with simulation data is made. In Sec. IV we consider the case of the model of C_{60} and in Sec. V we finally present our conclusions.

II. THEORY

Here we consider a simple fluid, i.e., a classical system of identical particles interacting via a potential $V(\mathbf{r}_1, \mathbf{r}_2, \ldots)$ that can be written as the sum of two-body, spherically symmetric terms

$$V(\mathbf{r}_1, \mathbf{r}_2, \ldots) = \sum_{i<j} v(r_{ij}) , \tag{1}$$

where $\mathbf{r}_1$, $\mathbf{r}_2$, ... are the positions of the particles, v is the two-body potential, and r_{ij} is the distance between two particles labeled i and j. Following a procedure that is widely adopted in liquid-state theories [1], we assume that the potential $v(r)$ can be split into a repulsive contribution $v_R(r)$ and an attractive one $w(r)$

$$v(r) = v_R(r) + w(r) . \tag{2}$$

The repulsive term $v_R(r)$ is very short ranged and contains the singular part of the interaction that gives rise to the excluded volume effect, while $w(r)$ is longer ranged and is responsible for criticality and liquid-gas separation. One assumes that the properties of the system in which only the contribution $v_R(r)$ is present are known, so that it can be regarded as an unperturbed or *reference* system. If $v_R(r)$ is very stiff, as in the case of the LJ potential, it is known that such a reference system can be represented by an "equivalent" hard-sphere fluid of a suitable diameter d. From this point we are going to assume that the reference system is the hard-sphere one of a given diameter, possibly temperature and density dependent, and that the equation of state and the radial distribution function $g(r)$ of the hard-sphere fluid are known. The aim of the theory is then to determine how the behavior of the system is modified once the attractive perturbation $w(r)$ has been taken into account. What is peculiar to HRT is the way in which the perturbation is treated: in order to describe accurately the effect of fluctuations, the attractive part of the interaction is introduced in the system gradually via a sequence of Q systems whose interaction potential $v_Q(r)$ is given by the sum of the reference term $v_R(r)$ and a perturbation $w_Q(r)$. The latter is defined by its Fourier transform $\widetilde{w}_Q(k)$ according to the expression

$$\widetilde{w}_Q(k) = \begin{cases} 0, & k < Q \\ \widetilde{w}(k), & k > Q , \end{cases} \tag{3}$$

where $\widetilde{w}(k)$ is the Fourier transform of the full attractive potential $w(r)$. The parameter Q plays the role of an infrared cutoff whose effect consists in depressing fluctuations on length scales larger than $1/Q$. In particular, when one has $Q = \infty$ the Q system coincides with the reference system, whereas for $Q = 0$ it coincides with the fully interacting one. The corresponding evolution of thermodynamics and correlations can be determined by means of perturbation theory and is described by an exact hierarchy of equations involving correlation functions of increasing order. Here we are interested in the first equation of the hierarchy, which gives the evolution of the Helmholtz free energy per unit volume A_Q of the Q system. This turns out to be governed by the perturbation $\widetilde{w}(k)$ and by the direct correlation function in momentum space $\widehat{c}_Q(k)$ of the Q system itself. This function is related to the structure factor $S_Q(k)$ by the algebraic relation

$$\widehat{c}_Q(k) = -\frac{1}{\rho S_Q(k)} , \tag{4}$$

where ρ is the density of the system. The direct correlation function we have adopted here differs from the usual one as defined by the Ornstein-Zernike relation [1] in that (4) includes also the ideal gas contribution, which in k space is just the constant additive term $-1/\rho$. We also introduce the quantity $\widetilde{\Phi}(k) = -\beta\widetilde{w}(k)$, where as usual we have set $\beta = 1/k_BT$, k_B being the Boltzmann constant and T the absolute temperature. The equation for the free energy then reads

$$\frac{\partial \mathcal{A}_Q}{\partial Q} = -\frac{Q^2}{4\pi^2} \ln\left(1 - \frac{\widetilde{\Phi}(Q)}{\widehat{\mathcal{C}}_Q(Q)}\right) . \tag{5}$$

In the above equation we have introduced a modified free energy $\mathcal{A}_Q$ and a modified direct correlation function $\widehat{\mathcal{C}}_Q(k)$ in order to eliminate some discontinuous contributions that appear in the physical quantities A_Q and $\widehat{c}_Q(k)$ due to the sharp cutoff adopted in the definition (3) of $\widetilde{w}_Q(k)$. These modified quantities are related to the physical ones by the expressions

$$\mathcal{A}_Q = -\beta A_Q - \frac{1}{2}\rho \int \frac{d^3\mathbf{k}}{(2\pi)^3} \left[\widetilde{\Phi}(k) - \widetilde{\Phi}_Q(k)\right] + \frac{1}{2}\rho^2 \left[\widetilde{\Phi}(0) - \widetilde{\Phi}_Q(0)\right] , \tag{6}$$

$$\widehat{\mathcal{C}}_Q(k) = \widehat{c}_Q(k) + \widetilde{\Phi}(k) - \widetilde{\Phi}_Q(k) . \tag{7}$$

In the $Q \to 0$ limit $\mathcal{A}_Q$ and $\widehat{\mathcal{C}}_Q(k)$ yield, respectively, the free energy A and the direct correlation function $\widehat{c}(k)$ of the fully interacting system, which are then recovered at the end of the evolution. For $Q = \infty$ instead, A_Q and $\widehat{c}_Q(k)$ are nothing but the corresponding quantities of the reference system A_R and $\widehat{c}_R(k)$ and the definitions (6) and (7) reduce to the well-known mean-field approximation for A and to the corresponding random-phase approximation for $\widehat{c}(k)$. Equation (5) then describes how the mean-field free energy is affected by the subsequent introduction of fluctuations. As already stated in the Introduction, the corresponding evolution of $\widehat{\mathcal{C}}_Q(k)$ and of higher-order correlations [7] will not be considered here, but we will restrict ourselves to Eq. (5). We then need a closure relation for $\widehat{\mathcal{C}}_Q(k)$. This function is subject to two main constraints, which are related respectively to the long- and the short-range behavior of the correlations in a fluid: first, the zero-wave-vector limit of the direct correlation function must be proportional to the inverse compressibility of the system due to the well-known compressibility rule. In terms of the modified quantities this condition reads

$$\widehat{\mathcal{C}}_Q(k=0) = \frac{\partial^2 \mathcal{A}_Q}{\partial \rho^2} . \tag{8}$$

Moreover, each Q system is affected by the singular interparticle repulsion due to the reference part of the interaction and hence it must satisfy the so-called *core condition*, i.e., the radial distribution function of the Q system $g_Q(r)$ must vanish for every Q whenever r is less than the

characteristic dimension d of the particles. If $g_Q(r)$ is expressed by the Fourier transform of the structure factor $S_Q(k)$ and Eq. (4) is used, one gets

$$1-\frac{1}{\rho}\int\frac{d^3\mathbf{k}}{(2\pi)^3}\,e^{i\mathbf{k}\cdot\mathbf{r}}\left[\frac{1}{\rho\,\hat{c}_Q(k)}+1\right]=0$$

$$\text{for } r<d \text{ and for every } Q\,. \quad (9)$$

The expression we have adopted for $\hat{\mathcal{C}}_Q(k)$ is the same used in Ref. [8], which reads

$$\hat{\mathcal{C}}_Q(k)=\hat{c}_R(k)+\lambda_Q\tilde{\Phi}(k)+\hat{\mathcal{G}}_Q(k)\,. \quad (10)$$

In (10) both λ_Q and $\hat{\mathcal{G}}_Q(k)$ must be regarded as functions of the density and temperature of the system. The quantity λ_Q is chosen so that the thermodynamic consistency condition (8) is satisfied, while $\hat{\mathcal{G}}_Q(k)$ is determined by the core condition (9); its inverse Fourier transform $\mathcal{G}_Q(r)$ is different from zero only for $r<d$. The closure (10) then resembles the ORPA approximation for the direct correlation function. However, we must notice that in our case this expression is coupled to the evolution equation (5) by the compressibility rule (8). Equation (5) then gives rise to a partial differential equation for the free energy $\mathcal{A}_Q$ involving both $\partial\mathcal{A}_Q/\partial Q$ and $\partial^2\mathcal{A}_Q/\partial\rho^2$. As has already been shown [7,8], the universal features of the theory in the critical region are not affected by the detailed form of the closure relation: in fact, the relevant information for universality is contained in the small-k limit of $\hat{\mathcal{C}}_Q(k)$. According to Eq. (10), this is always an analytic function of k, that is, the above expression for $\hat{\mathcal{C}}_Q(k)$ is an Ornstein-Zernike closure. For every closure of this kind the compressibility rule (8) implies that at small wave vectors one has

$$\hat{\mathcal{C}}_Q(k)\underset{k\to0}{\sim}\frac{\partial^2\mathcal{A}_Q}{\partial\rho^2}-b_Qk^2\,, \quad (11)$$

where b_Q is a regular function of Q, ρ, and T with a finite limit for $Q\to0$ even at the critical point. The Ornstein-Zernike ansatz (11) becomes obviously false in the physical limit $Q\to0$ at the critical point, where it implies $\hat{\mathcal{C}}_Q(k)\sim k^2$, thereby giving a vanishing value for the critical exponent η, but it can be nonetheless considered as a reasonable approximation due to the small value of η for a three-dimensional system. Equation (11), together with the evolution equation for the free energy (5), is enough to determine the critical exponents predicted by the theory [7] as well as the qualitative behavior in the broken symmetry region [10], which then turn out to be the same for every Ornstein-Zernike closure, irrespective of the short-range details.

The short-range part of the interaction and the core condition (9) must of course be taken into account in order to describe also the nonuniversal features of the fluid, especially at high density. In the present approach the implementation of the core condition poses some problems, since the integral equation (9) must be satisfied for every Q system from $Q=\infty$ to $Q=0$ and is coupled to the evolution equation (5). As is standard in ORPA, the function $\mathcal{G}_Q(r)$ is expanded in series of Legendre polynomials $P_n(r)$ in the interval $(0,d)$

$$\mathcal{G}_Q(r)=\sum_{n=0}^{\infty}u_n(Q)P_n(r)\,. \quad (12)$$

We then determine the equations for the evolution of the coefficients $u_n(Q)$: to this purpose, we make use of the specific form of $\hat{c}_Q(k)$ given by Eqs. (7) and (10) and differentiate Eq. (9) with respect to Q. To simplify the calculation an approximation is introduced, namely, in the Q derivative of $\hat{c}_Q(k)$ we disregard the long-wavelength contribution containing the isothermal compressibility of the Q system. This amounts to decoupling the short- and the long-range evolution of the correlations: such an approximation seems to be a reasonable one, as can be checked at the end of the calculation by verifying that the radial distribution function $g_Q(r)$ for $r<d$ is indeed small for every Q. The resulting equation for the coefficients $u_n(Q)$ is

$$\sum_{n=0}^{\infty}M_{jn}(Q)\frac{du_n}{dQ}=\frac{Q^2}{2\pi^2}\,\tilde{P}_j(Q)\,\frac{\tilde{\Phi}(Q)}{\hat{\mathcal{C}}_Q(Q)\left[\hat{\mathcal{C}}_Q(Q)-\tilde{\Phi}(Q)\right]}\,, \quad (13)$$

where we have indicated with $\tilde{P}_j(Q)$ the Fourier transform of the Legendre polynomial $P_j(r)$. Each of the coefficients $M_{jn}(Q)$ is in turn given as the solution of an ordinary differential equation: if we set $\tilde{\varphi}(Q)=\tilde{\Phi}(Q)/\tilde{\Phi}(0)$, we have

$$\frac{dM_{jn}}{dQ}=-\frac{Q^2}{2\pi^2}\,\tilde{P}_j(Q)\left[\tilde{P}_n(Q)-\tilde{\varphi}(Q)\tilde{P}_n(0)\right]\times\left[\frac{1}{\hat{\mathcal{C}}_Q{}^2(Q)}-\frac{1}{\left(\hat{\mathcal{C}}_Q(Q)-\tilde{\Phi}(Q)\right)^2}\right]\,. \quad (14)$$

At the beginning of the evolution process we have the following set of initial conditions:

$$u_n(Q=\infty)=0\,, \quad (15)$$

$$M_{jn}(Q=\infty)=\int\frac{d^3\mathbf{k}}{(2\pi)^3}\,\frac{1}{\hat{c}_R^2(k)}\times\left[\tilde{P}_n(k)-\tilde{\varphi}(k)\tilde{P}_n(0)\right]\tilde{P}_j(k)\,. \quad (16)$$

A detailed derivation of these equations has already been reported in Appendix A of Ref. [8]. Following a prescription that is widely adopted in ORPA calculations, the series in Eqs. (12) and (13) have been truncated after the first five terms.

The evolution equation (5) supplemented with the closure relation (10) and with the compressibility rule (8) and the equations (12)-(14) for the implementation of the core condition give rise to a closed system of differential equations, which has to be integrated numerically from $Q=\infty$ to $Q=0$ in order to obtain the properties of the fully interacting system at the end of the evolution. In particular, the numerical integration of the partial differential equation for the free energy resulting from

Eqs. (5), (8), and (10) is a nontrivial problem: as already stated in the Introduction, the main difficulty consists in devising an algorithm that proves to be reliable even below the critical temperature T_c, when strong singularities implied by phase coexistence set in. To this purpose the *explicit* finite difference method [13] employed in Ref. [8] is not well suited, since for $T < T_c$ the conditions imposed by the essential requirement of numerical stability become so severe that the method is of no practical use. It is therefore advisable to resort to an *implicit* finite difference algorithm, which has the great advantage of being unconditionally stable [13]. In general, for nonlinear partial differential equations the use of such an algorithm makes the numerical computation very complex and time consuming. However, as already seen in Refs. [9,10], in our case the problem can be considerably simplified once Eq. (5) has been cast in a quasilinear form [14]; this is easily achieved by a substitution of the unknown function in Eq. (5). Specifically, we have set

$$\ln\left(1-\frac{\tilde{\Phi}(Q)}{\hat{C}_Q(Q)}\right)=-\frac{\tilde{\Phi}(Q)}{\hat{c}_R(Q)+\hat{\mathcal{G}}_Q(Q)}+\tilde{\Phi}^2(Q)\,f_Q\,, \tag{17}$$

where $f_Q = f_Q(\rho,T)$ is the new unknown function. If in the closure relation (10) the parameter λ_Q is eliminated in favor of $\partial^2\mathcal{A}_Q/\partial\rho^2$ by means of the compressibility rule (8) and the resulting expression for $\hat{C}_Q(k)$ is used on the left-hand side of Eq. (17), the latter can be inverted to express $\partial^2\mathcal{A}_Q/\partial\rho^2$ in terms of f_Q,

$$\frac{\partial^2\mathcal{A}_Q^{\circ}}{\partial\rho^2}=\tilde{\Phi}(0)\left[1-\exp\left(-\frac{\tilde{\Phi}(Q)}{\hat{c}_R(Q)+\hat{\mathcal{G}}_Q(Q)}+\tilde{\Phi}^2(Q)\,f_Q\right)\right]^{-1}-\frac{\hat{c}_R(Q)+\hat{\mathcal{G}}_Q(Q)}{\tilde{\varphi}(Q)}+\hat{\mathcal{G}}_Q(0)+\hat{c}_R(0)\,. \tag{18}$$

By differentiating twice Eq. (5) with respect to ρ and by making use of Eqs. (17) and (18), one gets a partial differential equation in a quasilinear form for the function f_Q:

$$\tilde{\Phi}^2(Q)\,\frac{\partial^2 f_Q}{\partial\rho^2}=E(Q,f_Q,\hat{\mathcal{G}}_Q)\,\frac{\partial f_Q}{\partial Q}+F(Q,f_Q,\hat{\mathcal{G}}_Q)\,, \tag{19}$$

where the explicit form of the coefficients $E(Q,f_Q,\hat{\mathcal{G}}_Q)$ and $F(Q,f_Q,\hat{\mathcal{G}}_Q)$ can be straightforwardly determined, but will not be reported here. This equation must be supplemented with an initial condition at $Q=\infty$ and with two boundary conditions at low and high density; as noted above, at the beginning of the evolution of the Q systems the modified direct correlation function $\hat{C}_Q(k)$ coincides with the RPA value. From Eq. (17) one then gets

$$f_{Q=\infty}(\rho,T)=\frac{1}{2}\,\rho^2 \qquad \text{for every } \rho,T. \tag{20}$$

When the density ρ goes to zero, $\hat{C}_Q(k)$ is dominated by the divergent ideal gas contribution and the logarithm on the left-hand side of Eq. (17) vanishes. We have then the following boundary condition for f_Q:

$$f_Q(\rho=0,T)=0 \qquad \text{for every } Q,T. \tag{21}$$

At high density the ORPA approximation is very reliable, so we have identified f_Q with its ORPA value, i.e., we have assumed that the quantity λ_Q in Eq. (10) is unity. In this way we obtain

$$f_Q(\rho,T)=\frac{1}{\tilde{\Phi}^2(Q)}\ln\left(1-\frac{\tilde{\Phi}(Q)}{\hat{c}_R(Q)+\tilde{\Phi}(Q)+\hat{\mathcal{G}}_Q(Q)}\right)+\frac{1}{\tilde{\Phi}(Q)\left[\hat{c}_R(Q)+\hat{\mathcal{G}}_Q(Q)\right]} \qquad \text{for every } Q,\ T. \tag{22}$$

Thanks to its quasilinear structure, Eq. (19) with the conditions (20)–(22) can be solved with a predictor-corrector implicit algorithm [14] without a great computational effort. The use of Eq. (17) to cast Eq. (5) in a quasilinear form may seem someway odd with respect to the more natural choice of setting f_Q equal to the logarithm on the right-hand side of Eq. (5), but it allows one to eliminate some spurious divergences that would otherwise affect the coefficients $E(Q,f_Q,\hat{\mathcal{G}}_Q)$ and $F(Q,f_Q,\hat{\mathcal{G}}_Q)$ in Eq. (19) every time the Fourier transform of the attractive interaction $\tilde{\Phi}(Q)$ vanishes. The results for f_Q and $\hat{\mathcal{G}}_Q$ determined by Eqs. (19) and (12)–(14) are then inserted in Eq. (18) and in Eqs. (8) and (10) to yield the thermodynamic as well as the two-particle correlations of the system. Notice that a single run of integration gives the full isotherm, from the ideal gas region to the dense regime in the freezing region.

III. APPLICATION TO THE LENNARD-JONES FLUID

As a first application of the theory of the preceding section we have considered the Lennard-Jones potential

$$v_{\mathrm{LJ}}(r)=4\epsilon\left[\left(\frac{\sigma}{r}\right)^{12}-\left(\frac{\sigma}{r}\right)^{6}\right], \tag{23}$$

and the subdivision of $v_{\mathrm{LJ}}(r)$ in a repulsive and in an attractive part is performed according to the prescription due to Weeks, Chandler, and Andersen (WCA) [1]. We then have

$$v_R(r)=\begin{cases} v_{\mathrm{LJ}}(r)+\epsilon, & r<2^{1/6}\sigma \\ 0, & r>2^{1/6}\sigma, \end{cases} \tag{24}$$

$$w(r)=\begin{cases} -\epsilon, & r<2^{1/6}\sigma \\ v_{\mathrm{LJ}}(r), & r>2^{1/6}\sigma\,. \end{cases} \tag{25}$$

As explained above, the reference system is represented by an "equivalent" hard-sphere fluid whose diameter d depends both on density and on temperature of the orig-

inal fluid and is determined by the well-known rule again due to WCA [1]:

$$\int d^3\mathbf{r}\, y_{\rm HS}(r,d)\{\exp[-\beta v_R(r)] - \exp[-\beta v_{\rm HS}(r,d)]\} = 0\,, \quad (26)$$

where $v_{\rm HS}(r,d)$ is the potential of hard spheres of diameter d, while $y_{\rm HS}(r,d)$ is the corresponding "cavity" correlation function, related to the radial distribution function $g_{\rm HS}(r,d)$ by the relation

$$y_{\rm HS}(r,d) = \exp[\beta v_{\rm HS}(r,d)]\, g_{\rm HS}(r,d)\,. \quad (27)$$

The hard-sphere fluid can in turn be described by the Carnahan-Starling equation of state [1] and by the Verlet-Weis parametrization of the two-particle correlation function [15,16]. We use reduced units $T^* = k_BT/\epsilon$ and $\rho^* = \rho\sigma^3$.

The partial differential equation (19) for the unknown function $f_Q(\rho,T)$ defined in Eq. (17) is solved numerically in the density interval $\rho^* = 0 - 1$ with initial condition (20) at $Q = 80$. The boundary condition at $\rho^* = 0$, corresponding to an ideal gas, is given by Eq. (21), while at $\rho^* = 1$ we have assumed that the standard ORPA approximation is appropriate and this gives the value (22) for f_Q. We have verified that the result of integration is not affected in a significant way by the precise value of ρ^* where we put the high-density boundary condition and by the initial value of Q. The spacing of the density grid is equal to $\Delta\rho^* = 5 \times 10^{-4}$ and the evolution of f_Q with Q is followed by setting $Q = \ln(1 + e^{-t})$ with a step $\Delta t = 10^{-2}$. As the integration of f_Q proceeds, the ordinary differential equations (13) and (14) that implement the core condition are integrated. Temperature only enters in the function $\tilde{\Phi}(Q) = -\tilde{w}(Q)/k_BT$, so that the equations are integrated separately at each T. The output of the integration gives directly, via Eq. (18), the inverse compressibility over the full density range and integration over ρ gives the chemical potential, the pressure, and the Helmholtz free energy. Entropy is obtained from the increment of the free energy between two neighboring isotherms. The quantities $\lambda_{Q=0}$ and $\hat{\mathcal{G}}_{Q=0}(k)$ are obtained from Eqs. (8) and (10) and from Eq. (12) and they determine the direct correlation function in k space. The radial distribution function $g(r)$ is then obtained via the Ornstein-Zernike relation. Inspection of $g(r)$ when r is less than the hard-sphere diameter d shows that the approximate scheme used to implement the core condition [Eqs. (12)–(16)] is as accurate as a standard ORPA calculation using the same finite set of Legendre polynomials.

We have verified that when T is above the critical temperature, the results are essentially equal to those obtained previously in a computation in which the evolution equation was not reduced to a quasilinear form [8]. This represents a test of our numerical methods. Below T_c two typical isotherms are shown in Fig. 1; for the lower temperature we also report the results of the approximate equation of state obtained by Nicolas *et al.* [17] by fitting

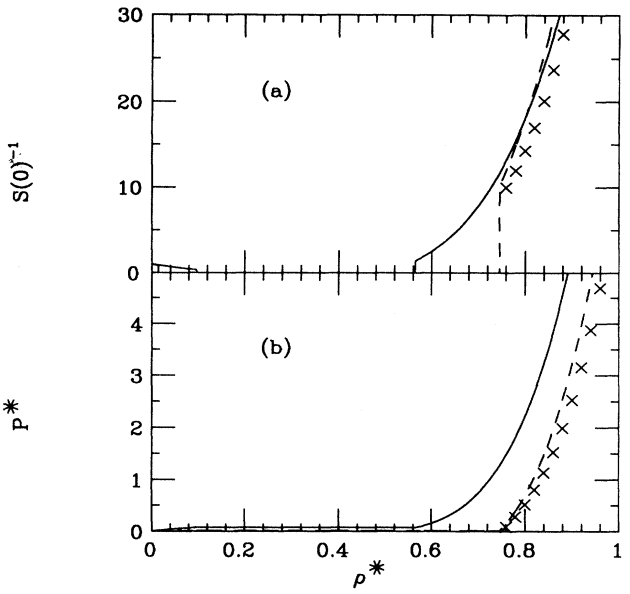

FIG. 1. (a) Inverse reduced compressibility and (b) vapor pressure of the Lennard-Jones fluid for two isotherms below the critical temperature of the system. $T^* = 1.2$, HRT (full curve); $T^* = 0.9$, HRT (dashed curve); and the Nicolas *et al.* equation of state [17] (×) results.

a large amount of data from simulations and virial series. The inverse isothermal compressibility is shown in Fig. 1(a) and the pressure in Fig. 1(b). We recall that the initial condition for the free energy at $Q = \infty$ corresponds to that of hard spheres supplemented by the attractive tail in mean-field approximation; at these temperatures P^* at $Q = \infty$ then displays a van der Waals loop and $S(0)$ is negative at intermediate density. Inclusion of fluctuation effects via the Q integration eliminates this unphysical behavior and it is found that as Q goes to zero, the inverse compressibility vanishes exponentially over a finite density range and, correspondingly, P^* has a horizontal part. No Maxwell construction has to be applied, but this result comes out from integration of the equation. The flat portion of the isotherms widens as T decreases and the boundary of this region of infinite compressibility gives the coexistence curve. The latter is shown in the ρ^*-T^* plane in Fig. 2 together with the diameter. We give also the HRT results when the core condition is not implemented, i.e., when the direct correlation function does not have the term $\hat{\mathcal{G}}_Q(k)$ in Eq. (10). The critical temperature is hardly affected by the core condition, but this has some effect on the critical density. The coexistence curve is in good agreement with the result of simulation [18]. In Fig. 2 we also show the result obtained from the MHNC integral equation [6]. There is an overall agreement, the HRT result being slightly closer to the simulation values. Let us remark that the MHNC does not have a proper critical point and numerically it has been found impossible to approach T_c closer than what is presented in the figure. The situation is quite different with HRT, which describes a true critical point with scaling behavior and nonclassical exponents. The HRT

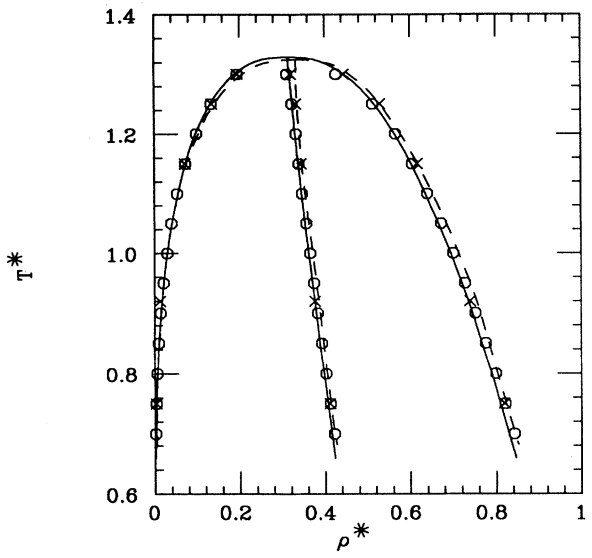

FIG. 2. Coexistence curve and diameter in the ρ^*-T^* plane. HRT (full curve), HRT without core condition (dashed curve), MHNC [6] (×), and simulation [18] (○) results.

equations can be solved numerically for temperatures arbitrarily close to T_c and the final limitation is just due to the adopted grid size in density.

The power-law behavior of the difference $\rho_l - \rho_v$ between the densities on the liquid and on the vapor side of the coexistence curve as a function of reduced temperature $t = (T_c - T)/T_c$ is demonstrated by the linear behavior in a bilogarithmic plot as shown in Fig. 3. From this analysis we locate the critical point at $T_c^* = 1.329$ and $\rho_c^* = 0.314$. These values are very close to the ones determined previously [8] ($T_c^* = 1.333$, and $\rho_c^* = 0.316$) from computations at $T > T_c$ by looking for the divergence of the isothermal compressibility, the slight change being due to the improved density mesh we have used now. In Table I the critical parameters given by HRT are compared with the predictions of other liquid-state

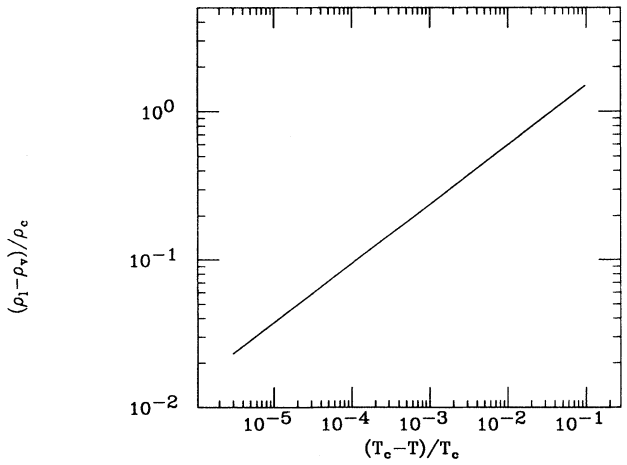

FIG. 3. Difference $(\rho_l - \rho_v)/\rho_c$ as a function of the reduced temperature $(T_c - T)/T_c$.

TABLE I. Critical parameters of the Lennard-Jones fluid. Both temperature and density are expressed in reduced units $T^* = k_B T/\epsilon$ and $\rho^* = \rho\sigma^3$. The HRT values are compared with the results of MHNC [6] and OCT [5] theories and with molecular dynamics (MD) simulation estimates [18].

Parameter	HRT	MHNC	OCT	MD
T_c^*	1.329	1.34	1.348	1.310
ρ_c^*	0.314	0.31	0.349	0.314

theories [5,6] as well as with the simulation values [18]. It can be seen that there is excellent agreement between the HRT and the simulation results, but one has to keep in mind the uncertainty in the simulation data due to the difficulty in locating a critical point from simulation on a finite system. The simulation value of the compressibility factor at the critical point is $Z_c = (P/\rho k_B T)_c = 0.306$, while HRT gives $Z_c = 0.323$. From the slope of the curve in Fig. 3 we obtain an exponent $\beta = 0.38$. This is close to the asymptotic value given by this theory, which is known to be $\beta = 0.345$, about 10% larger of the accepted value [7].

The coexistence curve in the ρ^*-P^* plane is shown in Fig. 4. The vapor pressure and the chemical potential as a functim of temperature along the coexistence curve are shown, respectively, in Figs. 5(a) and 5(b). All these quantities are in excellent agreement with the simulation results.

As already stated in the Introduction, HRT has a qualitatively wrong behavior exactly on the coexistence curve since it gives an infinite compressibility. This behavior does not appear on the scale of Fig. 1(a), where $1/S(0)$ seems to drop to zero almost discontinuously, but it shows up in an enlarged scale as in Fig. 6. An analytic study of the evolution equation [10] shows that $S(0)$ diverges as $a_{l,v}|\rho - \rho_{l,v}|^{-(4-D)/(D-2)}$ at the phase boundary, where D $(2 < D < 4)$ is the dimensionality of the system; for

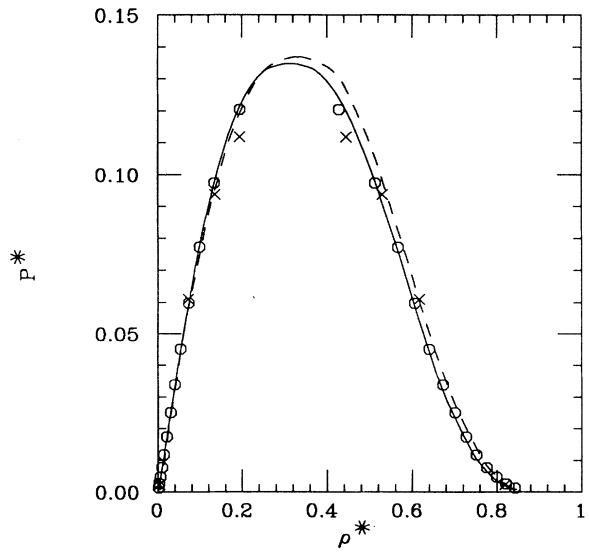

FIG. 4. Coexistence curve in the ρ^*-P^* plane. The graphic notation is the same as in Fig. 2.

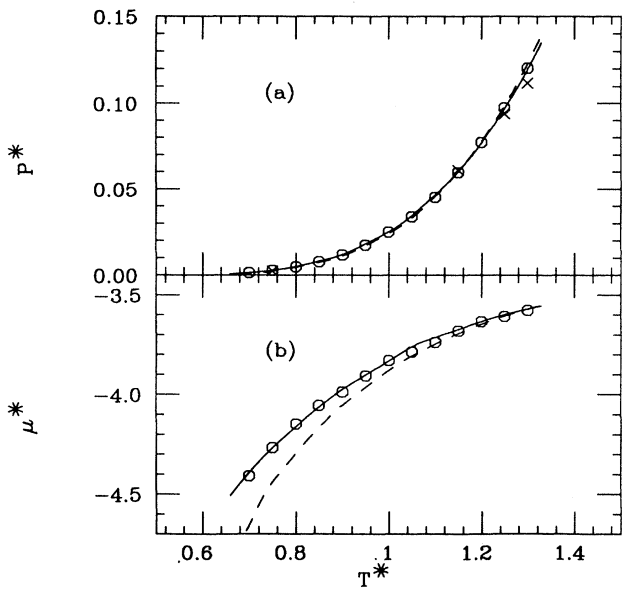

FIG. 5. Coexistence curve (a) in the T^*-P^* plane and (b) in the T^*-μ^* plane. The graphic notation is the same as in Fig. 2.

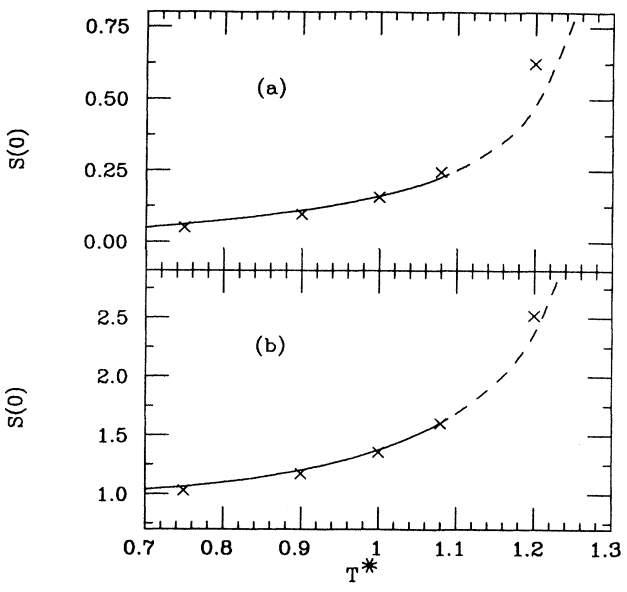

FIG. 7. Reduced compressibility on the (a) high-density and (b) low-density regions of the coexistence curve as a function of T^*. $S_{\rm true}(0)$ (×) [see Eq. (28)] and results of Nicolas *et al.* [17] (curve); the dashed portion of the curve refers approximately to the region where the equation of state of Nicolas *et al.* cannot be considered very reliable since the corresponding coexistence curve, obtained by means of a Maxwell construction, deviates appreciably from simulation results [18,19].

$D = 3$ this is a simple pole. The amplitudes a_l and a_v turn out to be related to the coefficient $b_{Q=0}$, which gives the curvature of the direct correlation function at convergence [see Eq. (11)] and can be computed straightforwardly once the value of b_Q on the coexistence curve has been determined. We can then assume that close to coexistence, $S(0)$ given by HRT consists of this spurious, divergent contribution, which is due to the adopted closure plus a genuine background term $S_{\rm true}(0)$, so that for densities outside the coexistence region $S_{\rm true}(0)$ can be estimated from

$$S_{\rm true}(0) = S(0) - a_{l,v}|\rho - \rho_{l,v}|^{-1} . \qquad (28)$$

We have verified that in the case of a three-dimensional lattice gas with nearest-neighbor attraction this procedure gives $S_{\rm true}(0)$ in close agreement with the correct value. For the present case the behavior of $1/S_{\rm true}(0)$ given by this prescription is shown along an isotherm in Fig. 6, where as before we report also the results for $1/S(0)$ obtained by the equation of state of Nicolas *et al.* Note that this equation can be continued analytically inside the coexistence region, whose boundaries must then be determined by resorting to a Maxwell construction. In Fig. 7 we report $S_{\rm true}(0)$ on the coexistence curve and again compare it with the prediction of Nicolas *et al.* We see that the agreement is good, except for the region close to the critical point, where, on the other hand, the coexistence curve as predicted by the aforementioned equation of state deviates appreciably from the most recent simulation results [19]. In fact, this equation cannot be probably considered very reliable in the near-critical regime due to its analytic behavior and to the values of its critical parameters ($T_c^* = 1.35$ and $\rho_c^* = 0.35$), which

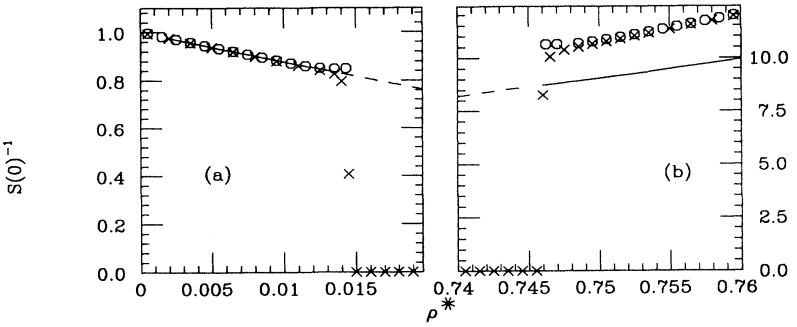

FIG. 6. Inverse reduced compressibility for the isotherm $T^* = 0.9$. Computed $1/S(0)$ (×), $1/S_{\rm true}(0)$ (○) [see Eq. (28)], and results from the equation of state of Nicolas *et al.* [17] inside (dashed curve) and outside (full curve) the coexistence region.

are significantly different from the commonly accepted ones [18].

We do not perform a comparison with experimental data on rare gases because the deviations would be mainly due to the approximate representation of the true interatomic interaction by the LJ potential. The comparison of the experimental data for krypton above T_c with the HRT results for an accurate pair interaction plus the three-body Axilrod-Teller interaction is found in Ref. [20]. It is possible to extend that computation to temperatures below T_c by applying the methods of the present paper, but we have not performed such a computation.

We consider now the HRT result for the radial distribution function $g(r)$ and the structure factor $S(k)$. As examples we consider two states close to the liquid branch of the coexistence curve, at $T^* = 1.36$ and $\rho^* = 0.5$ and at $T^* = 0.88$ and $\rho^* = 0.85$. The HRT results for $S(k)$ are shown in Fig. 8 together with the MHNC results. It is known that the MHNC gives quite an accurate correlation function. The main peak of $S(k)$ given by HRT is larger than the MHNC result by about 0.1. Also the subsequent oscillations of $S(k)$ have a larger amplitude for HRT. This last effect is due to the fact that our $S(k)$ has been computed for a hard sphere plus tail potential. We can reconstruct the $S(k)$ appropriate for a soft repulsive core by writing

$$g(r) = \exp\left[-\beta v_R(r)\right] y(r)\,, \tag{29}$$

where $y(r)$ is the cavity function for the hard sphere plus tail system given by HRT, and then transforming to k space. The resulting $S(k)$ is also shown in Fig. 8 and now is in good agreement with the MHNC result at large k. However, the main peak remains higher than the MHNC one and we can conclude that the correlation function given by the present HRT scheme is less accurate than the MHNC one. The comparison of $g(r)$ based on Eq. (29) with simulation [21] and with the MHNC is presented in Fig. 9. The agreement with simulation is better in the MHNC than in HRT.

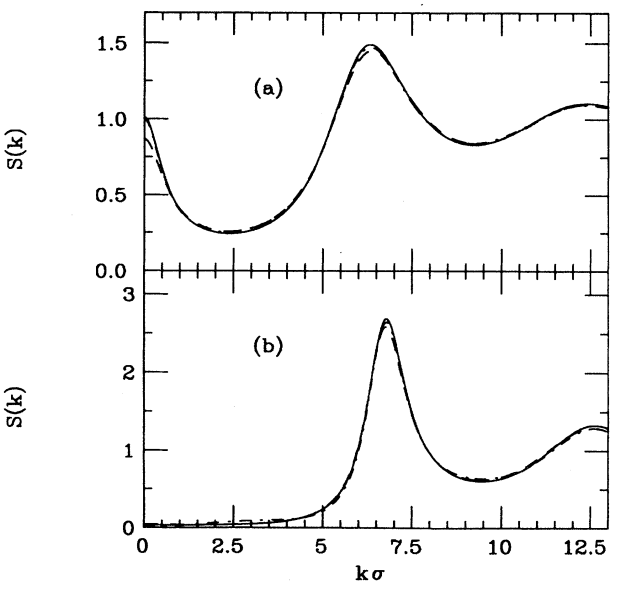

FIG. 8. Structure factor for the states (a) $T^* = 1.36, \rho^* = 0.5$ and (b) $T^* = 0.88, \rho^* = 0.85$. HRT (full curve), HRT as appropriate for a soft repulsive core according to Eq. (29) (dot-dashed curve), and MHNC (dashed curve).

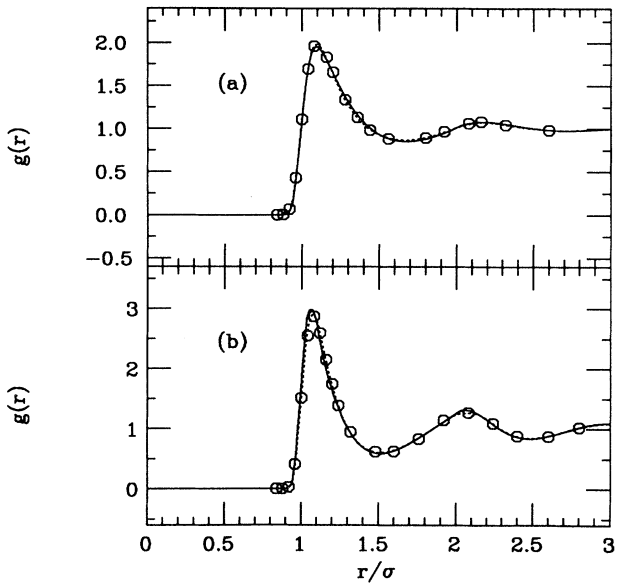

FIG. 9. Radial distribution function for the states (a) and (b) as in Fig. 8. HRT (full curve), MHNC (dotted curve), and simulation [21] (○) results.

IV. APPLICATION TO A MODEL INTERACTION FOR C_{60}

As another application of our theory we have considered the Girifalco potential [12]

$$v_G(r) = -\alpha\left[\frac{1}{s(s-1)^3} + \frac{1}{s(s+1)^3} - \frac{2}{s^4}\right] + \beta\left[\frac{1}{s(s-1)^9} + \frac{1}{s(s+1)^9} - \frac{2}{s^{10}}\right], \tag{30}$$

where $s = r/2a$, $2a = 0.71$ nm, $\alpha = 74.94 \times 10^{-15}$ ergs, and $\beta = 135.95 \times 10^{-18}$ ergs. This central potential has been used to model the interaction between C_{60} molecules at high temperature. There has been a specific interest to determine whether such a model has a critical point and a liquid branch or whether solidification preempts the liquid-vapor transition.

The Girifalco potential has a deeper and narrower attractive well when compared with LJ, as can be seen in Fig. 10, where the parameters σ and ϵ of the LJ potential have been chosen so as to be appropriate for C_{60} [22]. We have decomposed v_G with the same WCA rule used in Sec. III [Eqs. (24) and (25)] and the computation proceeds in a way similar to the LJ case. We find a critical point and the value of the critical parameters are given

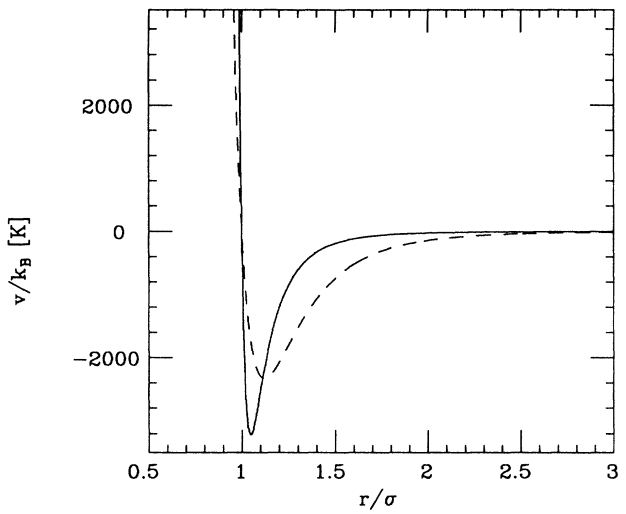

FIG. 10. Girifalco [12] (full curve) and Lennard-Jones [22] (dashed curve) interaction potentials. The distance σ at which the potential vanishes and the depth ϵ of the attractive well are equal to $\epsilon/k_B = 3218$ K, $\sigma = 0.959$ nm (Girifalco) and $\epsilon/k_B = 2330$ K, $\sigma = 0.922$ nm (Lennard-Jones).

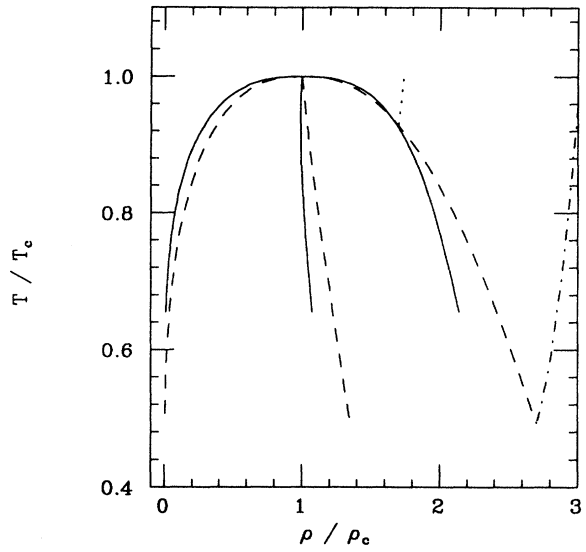

FIG. 11. HRT results for the coexistence curve and the diameter in the ρ/ρ_c-T/T_c plane. The graphic notation corresponds to the two potentials as in Fig. 10. The freezing transition is denoted by the dotted curve (Girifalco) and by the dot-dashed curve (Lennard-Jones).

in Table II. Some computations of the coexistence curve for the Girifalco potential have already been performed with integral equations; the corresponding results for the critical point are also reported in Table II together with estimates from numerical simulations. Our T_c is higher than the HMSA result [22] by 90 K and higher than the MHNC result [6] by about 200 K. It should be noted that these integral equations cannot be solved too close to T_c and quite a bit of extrapolation is needed to reach the critical point. From simulation data [22,23] the critical temperature has been estimated around 1800–1900 K, substantially smaller than our result, and for the critical density one computation has given a larger value [22] and another a smaller value [23]. In this latter case the critical point was present only as a metastable state. The coexistence curve given by HRT is shown in Fig. 11 together with that of the LJ fluid. It should be noted that at the critical point the effective hard-core packing fraction $\eta_c = \pi\rho_c d^3/6$, where d is the diameter of the effective hard core as given by (26), is substantially larger for the Girifalco potential ($\eta_c = 0.239$) than for the LJ potential ($\eta_c = 0.167$). This means that at the critical point the correlations for v_G are substantially stronger than in the LJ case; this is shown in Fig. 12, where $S(k)$ and $g(r)$ at the critical point in the two cases are plotted. The coexistence curve for v_G is less skewed toward high density in comparison to v_{LJ}.

Our theory does not describe the solidification transition so that in order to answer the question whether there is a liquid branch, we have to supplement HRT with a freezing criterion. We have adopted the simple but effective Verlet criterion [24]: solidification takes place when

TABLE II. Critical parameters of the Girifalco potential [see Eq. (30)] as predicted by HRT, HMSA [22], MHNC [6], and MD [22], and Monte Carlo (MC) [23] simulations. According to MC results the critical point should be only a metastable state of the system.

Parameter	HRT	HMSA	MHNC	MD	MC
T_c (K)	2138	2050	1920	1900	1798
ρ_c (nm^{-3})	0.50	0.56		0.56	0.42

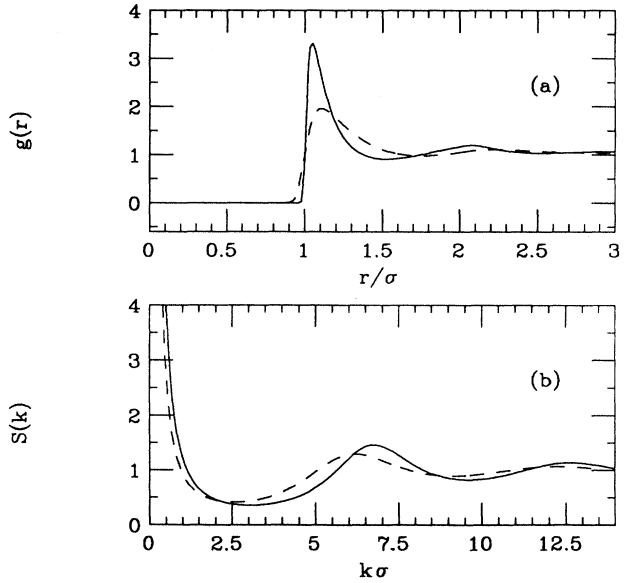

FIG. 12. (a) Radial distribution function and (b) structure factor at the critical point. The graphic notation is the same as in Fig. 10.

the main maximum of $S(k)$ reaches the value 2.85. Since HRT overestimates the height of $S(k)$ by about 0.1, we have implemented this freezing criterion with the value 2.95. This produces the freezing lines given in Fig. 11; the triple-point parameters for the LJ and the Girifalco potential are given respectively in Tables III and IV together with results from integral equations and simulations. For the Girifalco potential the triple-point temperature T_t is just 7% below T_c and ρ_t is 70% larger than ρ_c. The liquid branch is much more extended for the LJ interaction and the triple-point parameters are in reasonable agreement with simulation results [24]. In the case of v_G the simulation results give conflicting evidence. In one simulation [22] a triple point was found around $T_t \simeq 1800$ K and $\rho_t \simeq 1.0\,\mathrm{nm}^{-3}$, but no triple point was found in another simulation [23] and the liquid branch was present only as a metastable state. In the case of HMSA and MHNC integral equations the triple point has been located by means of an entropic criterion for freezing [6,22]. As can be seen from the data in Tables II and IV, there is an overall agreement that if the liquid branch exists at all, its extension is very limited.

HRT gives quite accurately the critical point of the LJ fluid but seems to strongly overestimate T_c for the Girifalco model. As discussed below, it is likely that the closure (10) we have adopted for the direct correlation function is less accurate for such a narrow and deep pair interaction and we are investigating a more appropriate form. On the other hand, the study of critical phenomena for a system with such a deep and narrow potential appears to be of some interest, although probably C_{60} is not the most suitable system in which to study these phenomena experimentally because T_c is too high to ensure stability of the C_{60} molecule and colloidal solutions appear more promising in this respect. In the standard case, correlations at the critical point are essentially gaslike, i.e., there is only a small amount of local order (see Fig. 12). On the contrary, the correlations are much more liquidlike when $v(r)$ is narrow and in fact in this case $g(r)$ at the critical point has a substantial amount of short range order, which then continues at larger distance with the slow decay characteristic of a critical point.

In order to analyze more quantitatively the influence of the short-range structure of a fluid on the location of the critical point, we can follow the numerical integration of Eq. (5), which describes the effects of fluctuations of wave vector Q on the free energy of the fluid. As already stated in Sec. II, the initial condition at $Q = \infty$ just represents the mean-field approximation, which is characterized by a "zeroth-order estimate" of the critical constants: $T^*_{\mathrm{MF}} = 1.42$ for the Lennard-Jones potential,

TABLE III. Triple-point parameters of the Lennard-Jones fluid. The notation is the same as in Table I. The HRT result is reported together with the values from HMSA [4] and MHNC [6] theories and from MC simulations [24]. See the text for the adopted freezing criterion.

Parameter	HRT	HMSA	MHNC	MC
T_t^*	0.66	0.66	0.63	0.68
ρ_t^*	0.85	0.86	0.86	0.85

TABLE IV. Triple-point parameters of the Girifalco potential. The notation is the same as in Table II. According to MC results the system should not have a triple point at all.

Parameter	HRT	HMSA	MHNC	MD	MC
T_t (K)	1979	1774	1620	$\simeq 1800$	
ρ_t (nm^{-3})	0.848	0.944	1.00	$\simeq 1.00$	

corresponding to $T_{\mathrm{MF}} = 3309$ K for LJ parameters fitted to C_{60} as in Fig. 10 and $T_{\mathrm{MF}} = 2275$ K for the Girifalco potential. The critical packing fraction in mean-field approximation is $\eta_{\mathrm{MF}} = 0.132$ in both cases. Quite generally, the effects induced by fluctuations are expected to be considerably more visible in systems characterized by shorter-range interactions. Long-wavelength fluctuations have been extensively discussed in the framework of the renormalization group and an approximate Ginsburg-like criterion can be consistently obtained also within our differential approach under the hypothesis that the different potentials are parametrized by a single dimensionless quantity R representing the ratio between the range of the attractive part and the size of the molecules. This Ginsburg criterion would predict a scaling of the form $(T_{\mathrm{MF}} - T_c)/T_{\mathrm{MF}} \sim R^{-3}$, leading to a decrease of the critical temperature in the Girifalco model three times larger than the one observed in the Lennard-Jones potential. Instead, the numerical integration of the differential equation predicts a moderate lowering of the critical temperature due to fluctuations (about 6%) in both cases, despite the considerable difference in the range of the interactions. A detailed analysis of the numerical solution of Eq. (5) shows that the shift in the critical temperature is actually due to two opposite and physically distinct effects: the well known, previously discussed reduction of T_c due to long-wavelength fluctuations and the increase of T_c induced by short-range order, i.e., corresponding to short-wavelength fluctuations of wave vector $Qd \sim 2\pi$, d being the effective hard-sphere diameter. These strongly affect the mean-field approximation for narrow attractive potentials in such a way that the effective critical temperature, before the introduction of long-wavelength fluctuations, turns out to be higher than the mean-field value. This effect is expected every time the interaction has nonnegligible Fourier components at short wavelengths and it is considerably more important for the Girifalco interaction potential than for the LJ one since the former shows a pronounced short-range structure in the critical region.

As already discussed, the ORPA-like closure of Eq. (5) adopted in the present analysis is known to overestimate the main peak of the structure factor at high density, leading to an artificial enhancement of the influence of short-wavelength fluctuations on the free energy of the model. As a consequence, the shift in critical temperature due to strong local order is also overestimated and for the Girifalco model this results in too high a value of the critical temperature itself. Instead, our approach accurately describes the effects due to long-wavelength fluctuations that dominate in the LJ-type interactions. A better analytical representation of the main peak of the

structure factor is therefore necessary in order to make HRT accurate also for deep and narrow potentials.

V. SUMMARY

In conclusion, we have presented results about the thermodynamics and the correlations in liquids throughout the phase diagram, with particular emphasis on the phase transition region: the critical point and the coexistence curve. The analysis has been carried out by use of the hierarchical reference theory of fluids together with an approximate ORPA-like closure that provides the momentum dependence of the direct correlation function of the fluid. The quality of the resulting correlation functions is therefore at least comparable to that of known and appreciated liquid-state theories. The accuracy in the thermodynamics is instead expected to be higher because the differential equation we have solved is formally exact, the only approximation being induced by the ORPA-like form of the correlation function used. This gives rise to comparable errors in the fluctuation corrections to the free energy rather than in the free energy itself. Our theory is particularly suitable for studying the phase transition region because near the critical point it shows the correct renormalization group structure, giving rise to scaling laws and nonclassical critical exponents. Inside the coexistence curve it reproduces rigorously flat isotherms without invoking the Maxwell construction.

HRT has been tested by the use of two different potentials: a standard Lennard-Jones potential, where extensive numerical results are available (including simulations), and a narrower potential proposed by Girifalco for C_{60} molecules. This investigation supplements an analogous study carried out for lattice models. We believe that the results obtained by HRT on the thermodynamics are generally accurate in the whole phase diagram, as can be inferred by the good agreement with available simulation data. The equation of state, compressibility, and coexistence curve are very well reproduced for the LJ fluid. The accuracy in the case of the Girifalco potential is more difficult to test because of the lack of precise alternative numerical estimates. In this case, however, the critical temperature seems to be overestimated by our method if compared to numerical simulations. The discrepancy may be attributed to the closure relation, linear in the attractive potential, which becomes less accurate for deeper and narrower potentials. The analysis of the fluctuation corrections to the location of the critical point allows us to identify two mechanisms responsible for the change in T_c with respect to a simple mean-field approximation: long-wavelength fluctuations depress the critical temperature, but the short-wavelength structure has the opposite effect, at least in the models studied here. Further studies leading to a precise determination of the critical temperature for narrow potentials are required in order to examine more thoroughly the influence of local order on the location of the critical point.

The correlation functions show more clearly the intrinsic limitations induced by the ORPA-like closure that has been adopted here: a splitting of the potential in attractive and repulsive contribution is first needed and then a mapping of the repulsive part onto a hard-sphere gas is also required in order to apply our formalism. These two steps lower the accuracy in the short range structure of the liquid, as can been shown by comparing ORPA to other liquid-state theories. The defects introduced by the mapping of the repulsive interaction onto hard spheres can be partly compensated by introducing the cavity correlation function $y(r)$, but this cannot be considered a fully consistent procedure and should be replaced by a more satisfactory treatment of the short-range potential. Again, the limitations of the simplified closure adopted in our investigation are emphasized in the Girifalco model, which shows a considerable short-range structure also in the critical region and reflect in the lower accuracy of HRT for this class of interactions. A noticeable improvement on the description of correlations within HRT will follow from a closure able to treat accurately continuous potentials, avoiding both the splitting of the interaction and the linearization of the attractive contribution.

ACKNOWLEDGMENTS

This work has been supported by Ministero dell'Università e della Ricerca Scientifica, by Istituto Nazionale di Fisica della Materia, and by Consiglio Nazionale delle Ricerche under Progetto Finalizzato "Sistemi Informatici e Calcolo Parallelo." We are grateful to C. Caccamo for having communicated to us the results of his MHNC calculations prior to publication and to A.Z. Panagiotopoulos for correspondence.

[1] See, for instance, J.P. Hansen and I.R.Mc. Donald, *Theory of Simple Liquids* (Academic, London, 1986).
[2] See, for instance, A. Parola and L. Reatto, Nuovo Cimento D **6**, 215 (1985).
[3] L. Belloni, J. Chem. Phys. **98**, 8080 (1993), and references therein.
[4] C. Caccamo, P.V. Giaquinta, and G. Giunta, J. Phys. Condens. Matter **5**, B75 (1993).
[5] S.H. Sung and D. Chandler, Phys. Rev. A **9**, 1688 (1974).
[6] C. Caccamo (private communication).
[7] A. Parola and L. Reatto, Phys. Rev. A **31**, 3309 (1985).
[8] A. Meroni, A. Parola, and L. Reatto, Phys. Rev. A **42**, 6104 (1990).
[9] D. Pini, A. Parola, and L. Reatto, J. Stat. Phys. **72**, 1179 (1993).
[10] A. Parola, D. Pini, and L. Reatto, Phys. Rev. E **48**, 3321 (1993).
[11] See, for instance, M.E. Fisher, Rep. Prog. Phys. **30**, 615

(1967).
[12] L.A. Girifalco, J. Chem. Phys. **96**, 858 (1992).
[13] See, for instance, W.H. Press, B.P. Flannery, S.A. Teukolsky, and W.T. Vetterling, *Numerical Recipes* (Cambridge University Press, Cambridge, 1986).
[14] See W.F. Ames, *Numerical Methods for Partial Differential Equations* (Academic, New York, 1977).
[15] L. Verlet and J.J. Weis, Phys. Rev. A **5**, 939 (1972).
[16] D. Henderson and E.W. Grundke, J. Chem. Phys. **63**, 601 (1975).
[17] J.J. Nicolas, K.E. Gubbins, W.B. Streett, and D.J. Tildesley, Mol. Phys. **37**, 1429 (1979).
[18] A. Lotfi, J. Vrabec, and J. Fischer, Mol. Phys. **76**, 1319 (1992).
[19] B. Smit, J. Chem. Phys. **96**, 8639 (1992).
[20] A. Meroni, L. Reatto, and M. Tau, Mol. Phys. **80**, 977 (1993).
[21] L. Verlet, Phys. Rev. **165**, 201 (1968).
[22] A. Cheng, M.L. Klein, and C. Caccamo, Phys. Rev. Lett. **71**, 1200 (1993).
[23] M.H.J. Hagen, E.J. Meijer, G.C.A.M. Mooij, D. Frenkel, and H.N.W. Lekkerkerker, Nature **365**, 425 (1993).
[24] J.P. Hansen and L. Verlet, Phys. Rev. **184**, 151 (1969).